

# Designing a W-type index praseodymium-doped chalcogenide fiber for strongly-efficient MIR Laser beyond 4 $\mu\text{m}$

Original Scientific Paper

## M A Khamis

Middle Technical University,  
Baquba Technical Institute, Electrical Techniques Department  
Muasker Al Rashid Street, Baghdad, Iraq  
mustafaelectronic@mtu.edu.iq

## Ziad QaisAlAbbasi

Middle Technical University,  
Baquba Technical Institute, Electrical Techniques Department  
Muasker Al Rashid Street, Baghdad, Iraq  
ziad.al-abbasi@mtu.edu.iq

**Abstract** – This study is to propose an efficient design based on W-type index praseodymium ( $\text{Pr}^{3+}$ )-doped chalcogenide fiber to enhance the emission of mid-infrared (MIR) wavelength beyond 4  $\mu\text{m}$ . The advantage of the proposed design is to enlarge the core diameter to 32  $\mu\text{m}$  under single mode guidance in order to restrict any impacts of nonlinearity and enhance the applied pumping power before the damage threshold. The effective mode field areas are about 979  $\mu\text{m}^2$  and 812  $\mu\text{m}^2$  at 4.5  $\mu\text{m}$  emitted MIR wavelength and 2.04  $\mu\text{m}$  pump wavelength, respectively. In the considered laser layout within this paper, a single pair of Fiber Bragg Gratings FBGs lay is adopted in the overlapping area of the emitting cross-sections parts of  $\text{Pr}^{3+}$  ions in the transitions ( ${}^3\text{F}_2, {}^3\text{H}_6 \rightarrow {}^3\text{H}_5$  and  ${}^3\text{H}_5 \rightarrow {}^3\text{H}_4$ ). This selected laser layout avoids the difficulties in the fabrication of concatenated FBGs in  $\text{Pr}^{3+}$ -doped chalcogenide glass fibers. In addition, the efficiency of the laser can be also enhanced at this laser layout by emitting two photons in MIR wavelengths from one excited ion. The simulation outcomes indicate the possibility to exceed 61% of slope efficiency at 4.5  $\mu\text{m}$  for 1 dB/m loss in the fiber.

**Keywords:** mid-infrared laser, chalcogenide glass material, praseodymium-doped fiber, W-index structure

## 1. INTRODUCTION

Recently, mid infrared (MIR) light sources beyond 4  $\mu\text{m}$  have drawn considerable interests for applications in many industrial and scientific applications, including medical diagnosis, gas sensing, atmosphere, defence, food security, environment monitoring, etc [1-4]. This is because their wavelength region has strong absorption strength of radiations, and covers the main atmospheric windows as well as many molecular gases, soil pollutants, toxic agents, water and breath components [5]. MIR wavelength range can be generated from several light sources such as optical parametric amplifiers [6], quantum cascade laser [7], supercontinuum [8] and a fiber laser [9-11].

Among others light sources, lanthanide ion doped fiber lasers are promising light sources in the MIR fluorescence between 3-5  $\mu\text{m}$  wavelength range. Praseodymium ( $\text{Pr}^{3+}$ ) has attractive characteristics in the MIR fluorescence among others lanthanide ions [12]. This is

due to an available pumping of  $\text{Pr}^{3+}$  from 2  $\mu\text{m}$  thulium diode fiber laser. In addition, the pumped absorption cross-section of  $\text{Pr}^{3+}$  is high as compared to other lanthanide ions. Furthermore, the overlapping emission source is represented by a cross sectional area that lies between two levels. The first level is  ${}^3\text{F}_2, {}^3\text{H}_6 \rightarrow {}^3\text{H}_5$  (3.3–4.7  $\mu\text{m}$ ), on the other hand, the second level is  ${}^3\text{H}_5 \rightarrow {}^3\text{H}_4$  (3.7–5.5  $\mu\text{m}$ ). Which yields to avoid the need of the cascade lasing approach and enhance the MIR emission. Finally,  $\text{Pr}^{3+}$  has a strong cross relaxation process, leading to excite three ions to manifold  ${}^3\text{H}_5$  by de-excitation of one ion to  ${}^3\text{F}_3$  manifold [13]. However, it is prerequisite to use host materials with low phonon energy and optical loss to release an efficient MIR light source from a  $\text{Pr}^{3+}$ -doped fiber and the promising candidate for this purpose is the chalcogenide glass [14]. This host material has attractive properties such as good rare earth ion solubility and high refractive index. Also, the light propagates through this glass material for a broad range of wavelengths (2-14  $\mu\text{m}$ ). However, the main

problem to release MIR laser from chalcogenide fiber is the low damage threshold in which limits the applied pump power [15].

For this purpose it is required to make the fiber core with a large mode field area to increase the possible value of the applied pumping power before reaching its damage threshold. Unfortunately, this way has a limitation due to the enlarging of the core diameter which in turn drives the conventional fiber to multimode guidance that degrades the beam quality. Another way to overcome this limitation is by applying double cladding pumping scheme [9]. Despite enlarging the mode field area of the pump, the total laser efficiency is still limited to only 18% due to a low confinement factor of the pump at this scheme. Another possible way to enlarge the mode area of Pr<sup>3+</sup>-doped chalcogenide is based on a photonic crystal fiber PCF [16]. Although, this fiber design offers more flexibility and optical characteristics than the conventional fiber but the fabrication and fused splices represent more challenges.

A W-type fiber is an alternative approach to overcome the above limitation and to enlarge the core area. This fiber profile has potential characteristics such as a dispersion-flattened fiber. In addition, it has a tight confinement mode, and as it evaluated around  $V = 3.8$ , it is possible to say it has a large V-parameter as compared to the value  $V = 2.405$  in the conventional fiber [8]. Having a large-valued V-parameter means it is practically possible to widen the fiber core diameters and, at the same time, maintaining the fiber operation to be in the single operation mode. In addition, it is easy to splice this fiber type with the standard step index fiber (SIF) and hence it becomes appropriate for all fiber laser systems. The W-type index structure has been already considered for ytterbium-doped fiber laser operating at 1.077  $\mu\text{m}$  [17], erbium-doped fiber amplifier at S-band [18], Neodymium-doped fiber laser at 914nm [19], and a bismuth-doped germanosilicate fiber laser in E band [20].

This study adopts Pr<sup>3+</sup>-doped chalcogenide fiber laser based on W-type index structure is designed for MIR emission beyond 4  $\mu\text{m}$ . The core of the proposed design has a diameter of around 32  $\mu\text{m}$ . In addition, the field area of the considered effective mode is about 979  $\mu\text{m}^2$  at 4.5  $\mu\text{m}$  laser wavelength, and it is valued as 812  $\mu\text{m}^2$  at 2.04  $\mu\text{m}$  pump wavelength while maintained intrinsically single mode operation. For the laser scheme, a cascade pumping scheme is avoided by operation in the overlapping transition wavelengths of a Pr<sup>3+</sup>-doped chalcogenide fiber where a single pair Fiber Brag Grating is selected at 4.5  $\mu\text{m}$  wavelength. Our results reflect that the laser power efficiency can be theoretically reached to 61% at 4.5  $\mu\text{m}$  of MIR emission with 1dB/m of fiber loss.

## 2. DESIGN AND THEORY

The proposed fiber design consists of three material layers with different refractive indices. The largest and lowest refractive indices are the core and the in-

ner cladding, respectively as shown in Fig. (1). The core layer is composed of Pr<sup>3+</sup>: GeAsGaSe glass material ( $n_1$ ), whilst the outer cladding region consists of GeAsGaSe-S glass material ( $n_3$ ). A suitable percentage around (0.8 atomic %) of Sulphur (S) is added instead of Selenium (Se) in the outer cladding layer to reduce the refractive index [21]. The inner cladding layer is also composed of GeAsGaSe-S glass material ( $n_2$ ) but with twice percentage of addition Sulphur instead of Selenium to that in the outer cladding to make the refractive index of this region the lowest one. Fig. 2 indicates the refractive indices for several aspects of the fiber against the wavelength value. In particular it includes the core, the inner cladding and outer cladding against various wavelength levels.

By considering the W-index fiber, the normalized frequency (V) can be expressed as [8]:

$$V = \frac{2\pi a}{\lambda} \times NA = \frac{2\pi a}{\lambda} \sqrt{n_1^2 - n_3^2} \quad (1)$$

Where  $a$  is the radius of the core region,  $\lambda$  is the operating wavelength, NA is the numerical aperture,  $n_1$  and  $n_3$  are the refractive indices of the core and outer cladding, respectively. This parameter is important to locate the cutoff wavelength of the proposed system where the operating wavelength must be higher than the specified cutoff wavelength. The W index fiber has large value of V-parameter about (3.8) under the condition of single mode. The advantage of this large value is to enlarge the core diameter and therefore the mode field area of the proposed fiber under single mode operation. In our proposed fiber, the core diameter is optimized to achieve the condition that the calculated V-parameter is lower than the value of 3.8 at single mode operation including the operating wavelengths range for the pump 2.04  $\mu\text{m}$  and laser emission 4.5  $\mu\text{m}$ . Fig. 3 shows the calculated V-parameter for both pump and laser wavelengths. The results indicate that 16  $\mu\text{m}$  is the larger core radius to keep the operation under single mode in the chosen wavelengths for the proposed W-index fiber.

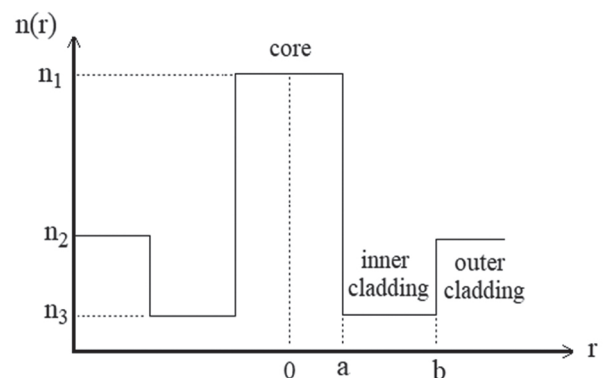
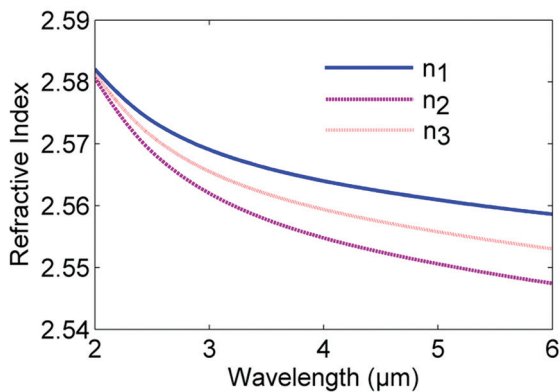


Fig. 1. Parameters structure of W-type fiber

A finite element method FEM that basison the idea of edge element is adopted in this paper for the computation of the guidance properties for the W-type

Pr<sup>3+</sup>-doped chalcogenide fiber laser [16]. The main advantages of applying FEM are to offer a mathematically elegant and rigorous formalism for modeling of complex geometrical shapes. In addition, a high degree of accuracy can be achieved with relatively short computation times. The propagation constant at the wavelengths 2.04 μm and 4.5 μm is calculated with three different refined meshes; with each newly generated mesh refinement possess a size that is half of the later one. Table (1) shows the computed convergence for the propagation factor with the mesh refinement approach. In the next simulation, the value of the propagation constant is obtained from the second mesh so as to provides the necessary level of accuracy for the subsequent calculations.



**Fig. 2.** The indices of refraction that belongs to the core, and both the inner cladding and the outer cladding against various wavelength levels.

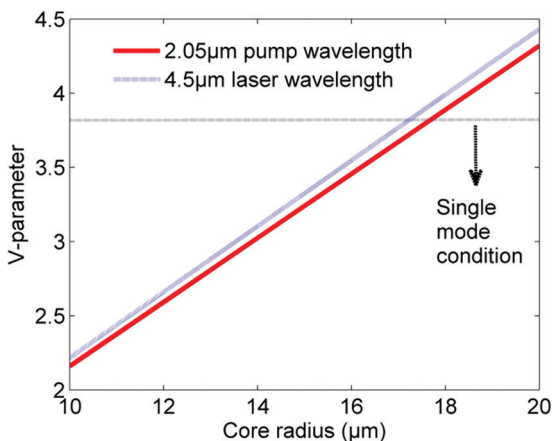


**Fig. 3.** The V-parameter calculated for the fiber of W-type at the pump and the laser wavelength with different core radius.

**Table 1.** The calculated propagation constant at pump wavelength 2.04 μm and laser wavelength 4.5 μm with two refined element meshes.

Mesh number	Propagation constant at 2.04 μm.	Propagation constant at 4.5 μm
280	$7.948994 \times 10^6$	$3.575330 \times 10^6$
1120	$7.949039 \times 10^6$	$3.575435 \times 10^6$
4480	$7.949037 \times 10^6$	$3.575434 \times 10^6$

At the fundamental mode, the electric field distribution is calculated at the pump wavelength 2.04 μm and laser emission 4.5 μm. Fig. 4 shows the distribution of the electric norm at 4.5 μm wavelength, the confinement of the optical field as clearly indicated in the doped area of the fiber.

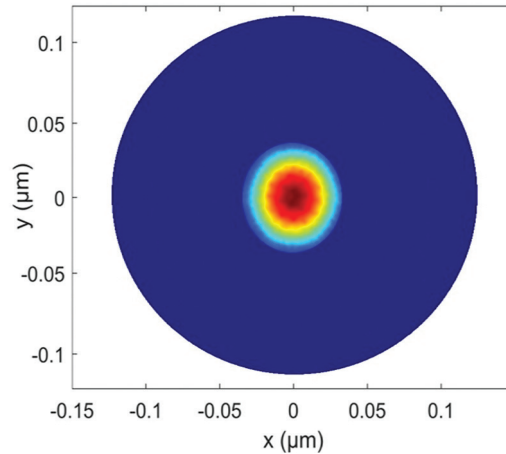


**Fig. 4.** The norm distribution depicted in fundamental mode of the electric field, where the wavelength is  $\lambda_s = 4.5 \mu\text{m}$ .

These calculated values of the electric field distribution are then exploited in the calculations of the field area of the effective mode as well as to obtain the factors of confinement at the operating wavelengths by applying the following expression [16]:

$$\Gamma_v = \frac{\iint_0^r |E_v^2(x, y)| dx dy}{\iint_0^\infty |E_v^2(x, y)| dx dy} \quad (2)$$

$$A_{eff} = \frac{\left( \iint_{-\infty}^\infty |E_v(x, y)|^2 dx dy \right)^2}{\iint_{-\infty}^\infty |E_v(x, y)|^4 dx dy} \quad (3)$$

Here  $v$  is to be substituted by either  $s$  for laser signal or  $p$  for pump, the radius doped area is denoted as  $r$ , the distribution of the electric field is represented by  $E_v(x, y)$  at a given signal and a specified pumping wavelengths. In our design of the W-type indexed fiber, the field area of the effective mode and the confinement factor are about 979 μm<sup>2</sup> and 0.63, respectively for the 4.5 μm wavelength. Moreover, they are valued about 812 μm<sup>2</sup> and 0.74, respectively for a wavelength of about 2.04 μm.

### 3. MODELLING OF THE FIBER LASER

In the case of a pump beam at 2.04 μm wavelength Pr<sup>3+</sup>-doped chalcogenide ions can be represented as three energy levels system [9]. Fig. 5 indicates the main ions interaction of Pr<sup>3+</sup>-doped chalcogenide at a low Pr<sup>3+</sup> concentration level. There are two different emission transition bands relevant to Pr<sup>3+</sup>-ions; namely, signal (1) (start-

ing from 3.3 up to 4.7  $\mu\text{m}$ ) between the manifolds ( ${}^3\text{F}_2, {}^3\text{H}_6 \rightarrow {}^3\text{H}_5$  and signal (2) (3.7–5.6  $\mu\text{m}$ ) between the manifolds  ${}^3\text{H}_5 \rightarrow {}^3\text{H}_4$ . As mentioned earlier in this article, there is an overlapping emission cross section between these two transition bands. In this study, the operating wavelength of the laser emission is chosen to be at 4.5  $\mu\text{m}$  which is located in the overlapping region of the emission transition (starting from 3.7 up to 4.7  $\mu\text{m}$ ). This way assists in avoiding the need of the cascade lasing approach in which is merely one pair of FBGs that would be required at 4.5  $\mu\text{m}$ .

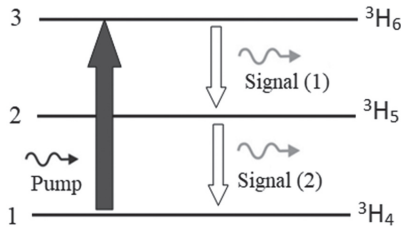


**Fig. 5.** Simplified energy level diagram for  $\text{Pr}^{3+}$

The population inversion of the energy levels can be computed from solving the rate equations model of  $\text{Pr}^{3+}$ -doped chalcogenide fiber laser. During the steady state, these equations can be described in the following algebraic equations form [9,12]:

$$\begin{bmatrix} a_{11} & a_{12} & a_{13} \\ a_{21} & a_{22} & a_{23} \\ 1 & 1 & 1 \end{bmatrix} \begin{bmatrix} N_1 \\ N_2 \\ N_3 \end{bmatrix} = \begin{bmatrix} 0 \\ 0 \\ N \end{bmatrix} \quad (4)$$

The equation coefficients can be expressed as follow:

$$a_{11} = w_{13}^p; a_{12} = w_{23}^s; a_{13} = -w_{31}^p - w_{32}^s - \frac{1}{\tau_3}$$

$$a_{21} = w_{12}^s; a_{22} = -w_{21}^s - w_{23}^s - \frac{1}{\tau_2}; a_{23} = w_{32}^s + \frac{\beta_{32}}{\tau_3}$$

Here  $\tau_2$  and  $\tau_3$  are the lifetime of the manifolds  ${}^3\text{H}_5$  and  ${}^3\text{H}_6$ , respectively; the transition branching ratio between  ${}^3\text{H}_6$  to  ${}^3\text{H}_5$  is denoted as  $\beta_{32}$ ;  $w_{13}^p$  and  $w_{23}^s$  are the pump stimulated rates;  $w_{23}^s$  and  $w_{32}^s$  are the signal (1) stimulated rates;  $w_{12}^s$  and  $w_{21}^s$  are the signal (2) stimulated rates. These rates can be expressed as:

$$w_{ij}^x = \frac{\Gamma_x \sigma_{ij} \lambda_x}{A h c} \times P_x \quad (5)$$

Here  $\Gamma_x$  and  $A$  refer to the confinement factor and effective mode area, respectively;  $x$  is either pump or signal (1) or signal (2);  $i$  and  $j$  are level transitions;  $\sigma_{ij}$  is the emission and absorption cross sections for specific  $ij$  transition. Finally,  $P_x$  is either substituted by the evolution power for pump or signal (1), otherwise it represents signal (2). Due to the operating wavelength at the overlapping region, so the power of signal (1) is the same at the signal (2). The spatial evolution of the pump  $P_p$  and signal  $P_s$  for all of the considered fiber length could be obtained from the solution of the following differential equations [12]:

$$\frac{dP_p^\pm}{dz} = \mp \Gamma_p \left[ \sigma_{pa} N_1 - \sigma_{pe} N_3 \right] P_p^\pm \mp \alpha P_p^\pm \quad (3)$$

$$\frac{dP_s^\pm}{dz} = \mp \Gamma_s \left[ (\sigma_{sa} N_2 - \sigma_{se} N_3) + (\sigma_{sa} N_1 - \sigma_{se} N_2) \right] P_s^\pm \mp \alpha P_s^\pm \quad (4)$$

Where  $\alpha$  is the fiber loss; - and + is the backward and forward travelling of the signal power and the boundary conditions that govern them are as follow:

$$P_s^+(0) = R_i P_s^-(0) \quad (5)$$

$$P_s^-(L) = R_o P_s^+(L) \quad (6)$$

Here  $L$  denotes the length of the laser cavity; Fiber Brag Grating reflectivity is denoted as  $R_i$  and  $R_o$ , where the former refers to for the input of the praseodymium-doped fiber and the later refers to the output. Equations (1)–(4) could be solved by applying the Relaxation algorithm approach. The signal power at the  $\lambda_s$  wavelength is propagated forth and back between the FBGs at the ends of the fiber. This process is iteratively repeated until the required accuracy meets the given conditions.

We apply the Relaxation approach to solve the pump differential equation eq.(6) and signal differential equation eq.(7). Table (2) summarizes all of the required parameters in the numerical investigation. It is assumed that the pump possesses loss levels and a signal wavelength to be 1 dB/m. This value exceeds the one adopted in the experimental investigations at the same host material [22].

**Table 2.** Values of numerical parameters used in the simulation set up [9, 12]

Quantity	Value	Unit
Lifetime of level 2	12	ms
Lifetime of level 3	4.2	ms
The concentration of $\text{Pr}^{3+}$ -ion	$5 \times 10^{25}$	$\text{m}^{-3}$
Branching ratio for the transitions between the level ${}^3\text{H}_6$ to ${}^3\text{H}_5$	0.42	
Signal (1) and Signal (2) wavelength	4.5	$\mu\text{m}$
Pump wavelength	2.04	$\mu\text{m}$
The field area of the effective mode at a certain pumping wavelength	812	$\mu\text{m}^2$
The field area of the effective mode at certain signal wavelength	979	$\mu\text{m}^2$
Confinement factor at the pump wavelength	0.73	
Confinement factor at the signal wavelength	0.62	
Absorption cross section at the pump wavelength	$2.2 \times 10^{-24}$	$\text{m}^2$
The cross section of the emission at the pump wavelength	$1.4 \times 10^{-24}$	$\text{m}^2$
The cross section of the emission at the signal (1) wavelength	$0.15 \times 10^{-24}$	$\text{m}^2$
The cross section of the absorption at signal (1) wavelength	$0.01 \times 10^{-24}$	$\text{m}^2$
The cross section of the emission at the signal (2) wavelength	$0.66 \times 10^{-24}$	$\text{m}^2$
Absorption cross section at the signal (2) wavelength	$0.75 \times 10^{-24}$	$\text{m}^2$

#### 4. RESULTS

After optimizing the core fiber diameter and computing both the factor of confinement as well as the field area of the effective mode, the laser performance of the suggested fiber can be now investigated for MIR emission at 4.5 $\mu\text{m}$  wavelength. The rate equations of the laser model can be solved numerically by using the data of table (2). Then, several vital parameters are investigated to examine the resulted performance, these parameters include the length of the laser cavity and the pumping power for Pr<sup>3+</sup>-doped chalcogenide laser based on W-type fiber. We assume that the proposed fiber laser is core pumped at one side while the MIR light is emitted from the other side. The input reflectivity is 0.05 and 0.95 for the pump and the signal, respectively whilst the reflectivity of the output FBG for the signal is 0.05. Firstly, the laser cavity length is investigated to find the optimized value. Fig. 6 displays the output laser power with the length of laser cavity at different values of the pump powers. It is clearly shown that the laser power increases in accordance with the increase of the cavity length for all the cases of the pump powers until reaching its maximum value, and then drops because of the fiber loss. The results also indicate that the required cavity length increases with the pump power and 0.7m is the optimized value at 1 W of the pump power and it is possible that more than 0.6 W of laser output power can be achieved at 4.5 $\mu\text{m}$  wavelength. The corresponding power intensity is about 1231MW/m<sup>2</sup>, which is much less than the applied values in the other previous literature studies.

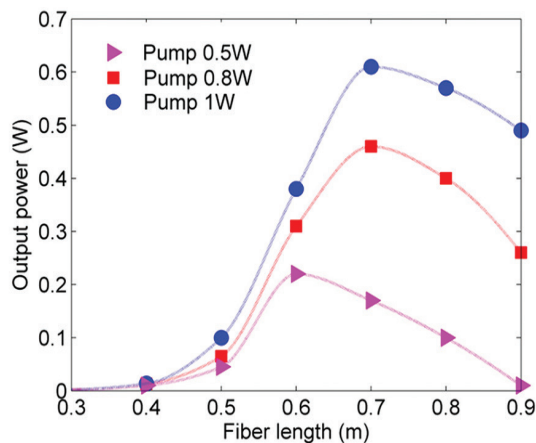


**Fig. 6.** The achievable output laser power as compared to the laser cavity-length evaluated at various

Next, the mechanism to obtain the efficiency of the laser slope is addressed, which is defined with the input pump power. In Fig. 7, an illustration of the dependency of the laser slope efficiency is depicted. This illustration is maintained upon the pumping power of two different fiber losses. The results indicate that more than 61% of slope efficiency is possible to achieve when the pump power is equal to 1W at fiber loss of 1dB/m. This slope drops to only 42% at the fiber loss

of 2dB/m. Thus, it is possible by applying our proposed fiber to get laser emission at 4.5 $\mu\text{m}$  with high levels of fiber losses.

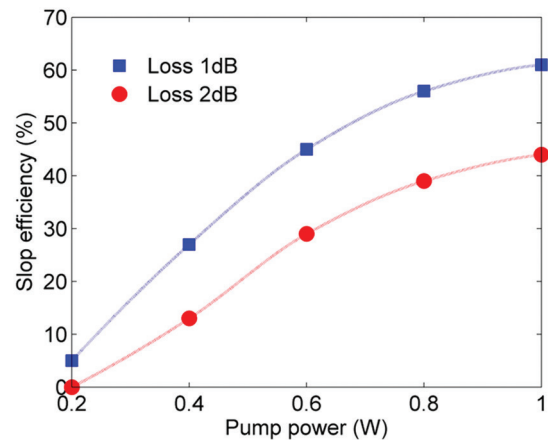


**Fig. 7.** The efficiency of the output slope against the applied pumping power measured at two values of fiber loss.

Another assessment of this paper is to evaluate the results of our design with the previously reported findings at MIR chalcogenide fiber lasers. We draw a comparison of W-type index pr<sup>3+</sup>-doped chalcogenide fiber laser with previously published results as illustrated in table (3). The results of our design exhibit high laser efficiency than the first three reported MIR sources with lower applied pump intensity. In spite of the fact that the PCF design produces the highest slope efficiency, this design still exhibits the disadvantages of high complexity in the fabrication and the splicing. As a result, our proposed W-type fiber offers a good and robust way to release an efficient MIR coherent source with less complexity in fabrication, design and splicing which is more suitable for the laser systems.

**Table 3.** Comparing the obtained simulation outcome against reported results in existing literature.

Layout of the laser	Area ( $\mu\text{m}^2$ )	Pumping intensity (MW/m <sup>2</sup> )	Efficiency of the slope
SIF with cascading laser concept [9]	2827	1768	16%
SIF with overlapped scheme [12]	2827	1768	48%
Multi-mode SIF based on resonant pumping design [15]	707	1414	54%
PCF with overlapping approach [16]	2050	500	64%
W- index type fiber with overlapping approach (current design)	812	1231	61%

## 5. CONCLUSIONS

In this study, a W-type index Pr<sup>3+</sup>-doped chalcogenide fiber laser has been proposed for MIR laser source at 4.5 μm wavelength. The proposed fiber exhibits the advantages of increasing the damage threshold of the pump power and restricting any nonlinearity effect by enlarging the effective mode field area. The proposed fiber consists of Pr<sup>3+</sup>: GeAsGaSe core glass, GeAsGaSe-S glass in both the inner and the outer cladding but with different atomic level of Sulphur (S). The FEM is adopted to simulate the distribution of the optical basic mode of a W-typed fiber. The field area of the effective mode is about 840 μm<sup>2</sup> at the pump 2.04 μm wavelength and 940 μm<sup>2</sup> at MIR laser wavelength 4.5 μm.

In the laser layout, we avoid the need of cascaded FBGs for MIR fiber laser by exploiting the characteristic of the overlapping region in the emitting cross-sections that belongs to the chalcogenide fiber that is doped with Pr<sup>3+</sup>. A single pair of FBGs is used at 4.5 μm wavelength for both signal (1) and signal (2). This laser layout is not only avoiding the fabrication complexity of cascaded FBGs but also increases the slope efficiency by emitting two photons in MIR wavelengths from one excited ion. The simulation findings indicate that at 4.5 μm wavelength, it could be seen that the realized slope efficiency exceeds more than 61% when the loss in the fiber is about 1 dB/m. As a result, our proposed W-type fiber is robust and represent an effective way to release an efficient MIR coherent source with less complexity in fabrication, design and splicing which is more suitable for all laser systems.

## 6. REFERENCES

- [1] V. A. Serebryakov, E. V. Boiko, N. N. Petrishchev, A. V. Yan, "Medical applications of mid-IR lasers problems and prospects", *Journal of Optical Technology*, Vol. 77, 2010, pp. 6-17.
- [2] A. B. Seddon, "Mid-infrared (IR) - A hot topic: The potential for using mid-IR light for non-invasive early detection of skin cancer in vivo", *Physica Status Solidi B*, Vol. 250, 2013, pp. 1020-1027.
- [3] F. Starecki et al. "Mid-IR optical sensor for CO<sub>2</sub> detection based on fluorescence absorbance of Dy<sup>3+</sup>: Ga<sub>5</sub>Ge<sub>20</sub>Sb<sub>10</sub>S<sub>65</sub> fibers", *Sensors and Actuators B: Chemical*, Vol. 207, 2015, pp. 518-525.
- [4] B. M. Walsh, H. R. Lee, N. P. Barnes, "Mid-infrared lasers for remote sensing applications", *Journal of Luminescence*, Vol. 169, 2016, pp. 400-405.
- [5] D. Caffey et al. "Recent results from broadly tunable external cavity quantum cascade lasers", *Proceedings Volume 7953, Novel In-Plane Semiconductor Lasers X*, 16 February 2011, p. 79531K.
- [6] M. Ebrahimzadeh, "Mid-infrared ultrafast and continuous-wave optical parametric oscillators", *Solid-State Mid-Infrared Laser Sources*, Springer, Berlin, Heidelberg, 2003, p.179.
- [7] A. A. Kosterev et al. "Methane concentration and isotopic composition measurements with a mid-infrared quantum-cascade laser", *Optics Letters*, Vol. 24, 1999, pp. 1762-1764.
- [8] M. A. Khamis, R. Sevilla, K. Ennser, "Design of W-Type Index Chalcogenide Fiber for Highly Coherent Mid-IR Supercontinuum Generation", *Journal of Lightwave Technology*, Vol. 36, 2018, pp. 5388-5394.
- [9] Ł. Sójka et al. "Study of mid-infrared laser action in chalcogenide rare earth doped glass with Dy<sup>3+</sup>, and Tb<sup>3+</sup>", *Optical Materials Express*, Vol. 2, 2012, pp. 1632-1640.
- [10] M. C. Falconi et al. "Design of an Efficient Pumping Scheme for Mid-IR Dy<sup>3+</sup>:Ga<sub>5</sub>Ge<sub>20</sub>Sb<sub>10</sub>S<sub>65</sub> PCF Fiber Laser", *IEEE Photonics Technology Letters*, Vol. 28, 2016, pp. 1984-1987.
- [11] S. D. Jackson, T. A. King, M. Pollnau, "Diode-pumped 1.7-W erbium 3-μm fiber laser", *Optics Letters*, Vol. 24, 1999, pp. 1133-1135.
- [12] M. A. Khamis, K. Ennser, "Design of Highly Efficient pr<sup>+3</sup>-doped Chalcogenide Fiber Laser", *IEEE Photonics Technology Letters*, Vol. 29, 2017, pp. 1580-1583.
- [13] L. D. Merkle, Z. Fleischman, E. E. Brown, J. L. Allen, U. Hommerich, M. Dubinskii, "Enhanced mid-infrared emission of ions in solids through a "3-for-1" excitation process – quantified", *Optics Express*, Vol. 29, 2021, pp. 39001-39015.
- [14] L. B. Shaw, B. Cole, P. A. Thielen, J. S. Sanghera, I. D. Aggarwal, "Mid-wave IR and long-wave IR laser potential of rare-earth doped chalcogenide glass fiber", *IEEE Journal of Quantum Electronics*, Vol. 37, 2001, pp. 1127-1137.
- [15] L. Sójka et al. "Numerical and experimental investigation of mid-infrared laser action in resonantly pumped doped chalcogenide fibre", *Optical and Quantum Electronics*, Vol. 49, 2017, p. 11426.
- [16] M. A. Khamis, R. Sevilla, K. Ennser, "Large Mode Area Pr<sup>+3</sup>-Doped Chalcogenide PCF Design for High Ef-

iciency Mid-IR Laser", IEEE Photonics Technology Letters, Vol. 30, 2018, pp. 825-828.

- [17] J. Kim, C. Codemard, Y. Jeong, J. Nilsson, J. K. Sahu, "High power continuous-wave Yb-doped fiber laser with true single-mode output using W-type structure", Proceedings of the Conference on Lasers and Electro-Optics/Quantum Electronics and Laser Science Conference and Photonic Applications Systems Technologies, Technical Digest, Long Beach, CA, USA, 21-26 May 2006.
- [18] M. A. Arbore, Y. Zhou, H. Thiele, J. Bromage, L. Nelson, "S-band erbium doped fiber amplifiers for WDM transmission between 1488 and 1508 nm", Proceedings of the OFC 2003 Optical Fiber Communications Conference, Atlanta, GA, USA, 28 March 2003.
- [19] S. Yoo et al. "Analysis of W-type waveguide for Nd-doped fiber laser operating near 940 nm", Optics Communications, Vol. 247, 2005, pp. 153-162.
- [20] A. S. Vakhrushev et al. "W-type and Graded-index bismuth-doped fibers for efficient lasers and amplifiers operating in E-band", Optics Express, Vol. 30, 2022, pp. 1490-1498.
- [21] Z. Tang et al. "Mid-infrared photoluminescence in small-core fiber of praseodymium-ion doped selenide-based chalcogenide glass", Optical Materials Express, Vol. 5, 2015, pp. 870-886.
- [22] G. E. Snopatin, V. S. Shiryayev, V. G. Plotnichenko, E. M. Dianov, M. F. Churbanov, "High-purity chalcogenide glasses for fiber optics", Inorganic Materials, Vol. 45, 2009, pp. 1439-1460.